

# Quantifying short chain branching microstructures in ethylene 1-olefin copolymers using size exclusion chromatography and Fourier transform infrared spectroscopy (SEC–FTIR)

Paul J. DesLauriers\*, David C. Rohlfing, Eric T. Hsieh

*Chevron Phillips Chemical Company LP, Bartlesville, OK 74004, USA*

Received 11 May 2001; received in revised form 27 July 2001; accepted 31 July 2001

## Abstract

A rapid method for the SEC–FTIR analysis of short chain branching distribution (SCBD) across the molecular weight distribution (MWD) is described and its application demonstrated using ethylene 1-olefins copolymers. Chromatograms are generated using the root mean square absorbance over the 3000–2700  $\text{cm}^{-1}$  spectral region (i.e. FTIR serves as a concentration detector). Spectra from individual time slices of the chromatogram are subsequently analyzed for comonomer branch levels using chemometric techniques. Furthermore, we are able to estimate error in the reported SCB content of each slice. Using the appropriate training sets, chemometric models can be constructed which provide SCB versus MWD profiles with sufficient precision to detect trends resulting from catalyst and process changes in LDPE and/or HDPE samples. We demonstrated the method by showing the results of a model that has enabled us to accurately quantify branching levels in polyolefins within  $\pm 0.5/1000$  total carbons (i.e. ca. 0.1 mol%) in samples with relatively low levels of SCB (i.e. <10 SCB/total carbons) and mixed branch types. © 2001 Published by Elsevier Science Ltd.

*Keywords:* Ethylene copolymers; Short chain branching; Chemometric techniques

## 1. Introduction

A critical technical support needed for polyolefin characterization is the profiling of short chain branching (SCB) across the polymer's molecular weight distribution (MWD). While broadening MWD is the key for improving processability, engineering SCB distribution over MWD is the essence for improving product performance. For example, given similar MW/MWD and density, polyethylene (PE) copolymer product properties such as environmental stress crack resistance (ESCR) can be greatly enhanced by preferentially placing the SCBs in the higher MW molecules [1].

A robust compositional analysis of ethylene 1-olefin copolymers involves both solvent and thermal fractionation of the sample. Each fraction is then characterized by size exclusion chromatography (SEC) to obtain molecular weight data and NMR spectroscopy to obtain SCB information. Although the resulting information on polymer composition is highly comprehensive, the efforts to acquire the wanted data are labor and time intensive. Less refined,

but faster analysis methods (several samples a day) for these desired distributions using SEC and Fourier transform infrared spectroscopy (FTIR) have been reported [2–7].

Two types of SEC–FTIR methods are typically used. In one method, sample eluent from the SEC column is deposited on a rotating germanium disk [2]. The solid deposit is subsequently analyzed offline by FTIR for branching content using absorption bands associated with the C–H deformation (bending) and/or  $\text{CH}_2$  rocking modes [3]. Conversely, in online FTIR methods [4–7], branching levels in the SEC eluent are measured in a heated flow cell. Measurements are made in the trichlorobenzene mobile phase and rely on C–H stretching bands found between 3000 and 2800  $\text{cm}^{-1}$ .

In this work, we describe an online, SEC–FTIR method for the analysis of short chain branching distribution (SCBD) over the MWD in ethylene 1-olefin copolymers that contain ethyl and/or butyl branching. A particular focus of this study was the use of multivariable statistical techniques for data analysis. The methodology for this analysis is presented and limitations that have been noted are addressed.

\* Corresponding author. Tel.: +1-918-661-7389; fax: +1-918-662-6072.  
E-mail address: deslapj@cpchem.com (P.J. DesLauriers).

## 2. Experimental

### 2.1. SEC–FTIR measurements

Samples of fractionated and commercial resins were dissolved in 1,2,4-trichloro-benzene (TCB) by heating the mixture for 2 h at 155°C in a Blue M, air convection oven. 2,6-di-tert-butyl-4-methylphenol (BHT) was added to the mixture in order to stabilize the polymer against oxidative degradation. The BHT concentration was 0.034 wt%.

A PL 210 SEC high temperature chromatography unit (Polymer Laboratories) equipped with two PLgel 10  $\mu\text{m}$  Mixed A or B columns (Polymer Laboratories) was used for molecular weight determinations. Samples were chromatographed at 1 ml/min using TCB as the mobile phase. The sample injection volume was 500  $\mu\text{l}$ . Samples were introduced to the FTIR detector via a heated transfer line and flow cell (KBr windows, 1 mm optical path, and ca. 70  $\mu\text{l}$  cell volume). The temperatures of the transfer line and flow cell were kept at  $143 \pm 1$  and  $140 \pm 1^\circ\text{C}$ , respectively. Perkin–Elmer FTIR spectrophotometers (PE 2000 and Spectrum One) equipped with narrow band mercury cadmium telluride (MCT) detectors were used in these studies.

All spectra were acquired using Perkin–Elmer Timebase software. Background spectra of the TCB solvent were obtained prior to each run. All IR spectra were measured at 8  $\text{cm}^{-1}$  resolution (16 scans). Chromatograms were generated using the root mean square absorbance over the 3000–2700  $\text{cm}^{-1}$  spectral region (i.e. FTIR serves as a concentration detector). Molecular weight calculations were made as previously described using a broad molecular weight PE standard [8]. Spectra from individual time slices of the chromatogram are subsequently analyzed for comonomer branch levels using chemometric techniques.

All spectra used in the studies described below in Sections 2.2 and 2.3 were taken at sample concentrations which far exceeded that needed for good signal to noise (i.e.  $>0.08 \text{ mg ml}^{-1}$  at the detector).

### 2.2. Spectrographic methods

Spectrum™ for Windows (Perkin–Elmer) software was used to obtain derivative and Fourier self deconvolution spectra. Derivative spectroscopy was used to estimate the number of components and their positions in sample FTIR spectra. Grushka and Monacelli [9] pointed out that the intensity ratio of the positive and negative lobes of the second derivative is a measure of band shape. For example, the ratios for Lorentzian and Gaussian bands are 0.25 and 0.446, respectively. We measure a ratio of 0.33 for the methylene asymmetric stretch in the derivative spectra of a high molecular weight ( $2.5 \times 10^6 \text{ g/mol}$ ) and narrow polydispersed ( $M_w/M_n = 1.3$ ) PE homopolymer sample. Based on this result, peak shapes used in our study were assumed to be part Lorentzian and part Gaussian. A Voigt equation was chosen to represent this peak shape. Peakfit™ (ver. 4,

Jandel Scientific) software was used to curve fit sample spectra. Fourier self-deconvolution spectra were generated using a Bessel filter, Gamma = 0.85 and length set to zero.

Digitally generated spectra used for model evaluations were made from SEC–FTIR acquired spectra. Spectra from the following polymers were used: poly (1-butene); 250 Me/1000 total carbons (TC), poly (1-hexene); 167 Me/1000 TC, an ethyl-branched PE fraction; 32 Me/1000 TC, butyl-branched PE fractions; 32 and 69.8 Me/1000 TC, and PE homopolymer fractions; 0.5 and 1.3 Me/1000 TC. All digitally generated spectra were made via the spectral calculation function supplied in Spectrum™ for Windows 1 software (Perkin–Elmer). Spectra with various branch levels were generated by normalizing spectra by area (3000–2760  $\text{cm}^{-1}$ ), multiplying them by the desired fractional amounts and subsequently combining the desired spectra together so that the final area was equal to one. For example, a spectrum representing a sample with a total methyl content of 35.6 Me/1000 TC was generated by first multiplying the normalized spectra from a highly branched PE fraction (69.8 Me/1000 TC) and a PE homopolymer fraction (1.3 Me/1000 TC) by 0.5, then adding the two spectra together.

### 2.3. Determination of branching

Narrow molecular weight ( $M_w/M_n \sim 1.1$ –1.3), solvent gradient fractions of ethylene 1-butene, ethylene 1-hexene, PE homopolymers, and low molecular weight alkanes were used in calibration and verification studies. The total methyl content of these samples ranged from 1.4 to 82.7 Me/1000 TC. Methyl content of samples was calculated from  $M_n$  or measured using C-13 NMR spectroscopy. C-13 NMR spectra were obtained on 15 wt% samples in TCB using a 500 MHz Varian Unity Spectrometer run at 125°C as previously described [10]. Methyl content per 1000 carbons by NMR was obtained by multiplying ( $\times 1000$ ) the ratio of total methyl signals to total signal intensity.

A partial least squares (PLS) calibration curve was generated using Pirouette chemometric software (Infometrix) to correlate changes in the FTIR absorption spectra with calculated or NMR measured values for methyls/1000 total carbons for the 25 samples. The FTIR absorption spectra used in the calibration model were made from co-added spectra collected across the whole sample. Only a portion of the spectral region (2996 and 2836  $\text{cm}^{-1}$ ) was used in the calibration step in order to minimize the effects of residual solvent absorption. Preprocessing of spectral data included area normalization, taking the first derivative of the spectra and mean centering all data. A three-component calibration model was calculated and optimized using the process of cross validation (RSQ = 0.999, SEV = 0.5). Outlier detection for individual measurements was generated from probability values obtained through the Pirouette chemometric software. Samples having probabilities  $>0.99$  were considered outliers.

Short chain branching levels were calculated by subtracting out methyl chain end contributions. The number of methyl chain ends ( $N_E$ ) was calculated (Appendix A) using the equation

$$N_E = (14,000)(2 - V_{CE})/M.$$

In this equation,  $V_{CE}$  is the number of vinyl terminated chain ends and  $M$  is the molecular weight calculated for a particular slice of the MWD. Typically, chain termination in chromium catalyzed resins results in the formation of a vinyl moiety [11]. Conversely, methyl chain ends are formed in the chain termination step of Zeigler–Natta catalyzed resins [12]. Therefore, in the above equation  $V_{CE}$  is assigned 1 for chromium catalyzed resins and 0 for Zeigler–Natta catalyzed resins. Also, the assumption is made that end group types (i.e. methyl or vinyl) remain fixed through out the MWD. Negative values for methyls/1000 total carbons that may result from over correction for methyl chain ends at low branching levels are given values of zero.

### 3. Results and discussion

#### 3.1. Spectral aspects of the measurement

Unlike solid state FTIR, where absorption bands associated with the C–H deformation (bending) and rocking modes are monitored for structural analysis purposes, FTIR detection of branching for PE in trichlorobenzene solutions relies on methyl and methylene absorption bands found between 3000 and 2800  $\text{cm}^{-1}$ . In this region of the spectrum, the chromatographic solvent used has the minimal amount of interfering absorption.

Studies of paraffin hydrocarbons by Fox and Martin [13] demonstrated that absorption bands at 2855 and 2928  $\text{cm}^{-1}$  are due to symmetrical and asymmetrical C–H stretching methylene ( $\text{CH}_2$ ) groups, respectively. In addition to these two bands, a shoulder at  $\sim 2900 \text{ cm}^{-1}$  was detected on the side of the 2928  $\text{cm}^{-1}$  methylene peak. Although we cannot confirm yet the assignment of this band, we speculate that it is combination absorption, possibly arising from  $\text{CH}_2$  deformation bands at 1440  $\text{cm}^{-1}$  (Raman-active) and 1460  $\text{cm}^{-1}$  (IR-active) as suggested by Nielsen et. al., for the solid state IR analysis of PE [14]. All three methylene vibrations are illustrated in the peak-fitted, PE spectrum given in Fig. 1a. The raw spectrum was obtained during the SEC–FTIR analysis of a high molecular weight ( $2.5 \times 10^6 \text{ g/mol}$ ) and narrow polydispersed ( $M_w/M_n = 1.3$ ) sample. The spectrum was taken at the peak of the chromatogram and represents a very narrow slice of the overall sample (i.e.  $M_p = M_n$  for the portion of sample in the slice). As such, this sample has a very low concentration of methyl chain ends (0.02 Me/1000 TC) and therefore its spectrum can be viewed as representing absorptions that solely arise from backbone methylene units.

The respective symmetrical and asymmetrical vibrations

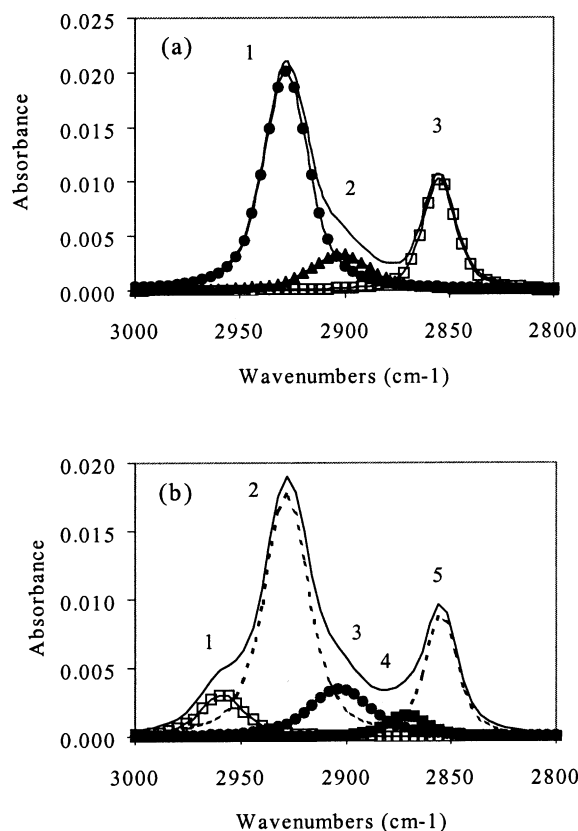


Fig. 1. Observed vibrations for peak fitted, SEC-FTIR spectra of high molecular weight polyethylene (a) and octacosane (b).

for methyl groups [13] at 2874 and 2957  $\text{cm}^{-1}$  are illustrated in the SEC–FTIR spectrum of octacosane (Fig. 1b). A comparison of spectra in Fig. 1 reveals that upon introducing the methyl structural units, a decrease in the methylene absorptions results. Typically, in long chain paraffins, the intensities of the  $\text{CH}_2$  and  $\text{CH}_3$  bands are directly related to the proportions of these groups present and the intensities of the  $\text{CH}_2$  bands change by a steady increment for each unit in chain length. Zenker [15] assumed the methyl absorption remained constant in straight chain hydrocarbons (C7 to C20) and found a linear relationship between the intensity ratio measured between methylene and methyl groups and the number of methylene units in the chain. The amount of  $\text{CH}_2$  moieties increases until an asymptotic relationship is reached.

From our analysis of several straight-chain hydrocarbons and low molecular weight PE samples (homopolymer fractions), we find that methyl chain-ends on polymers with  $M_n > 9000$  contribute little to the visible complexity of the spectrum. Similar conclusions were reached by Markovich et al. [6]. In this current study, we examined the spectra of polymers with various levels of ethyl and butyl short chain branches. When methyl moieties appear as chain ends to short chain branches, spectral profiles similar to those found for straight-chain hydrocarbons are observed (i.e. at least five main peaks). Also present in the case of

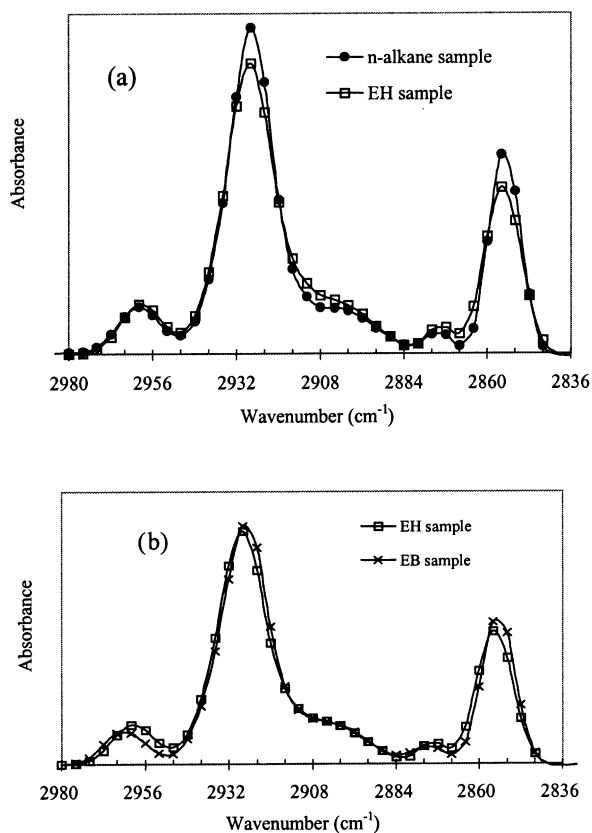


Fig. 2. Fourier self deconvolution spectroscopy for: (a) *n*-alkane and ethylene1-hexene samples, (b) ethylene1-hexene and ethylene1-butene samples. All samples contain  $\sim 70$  Me/1000 TC.

branched polyolefins is a weak-CH stretching vibration at  $\sim 2900$   $\text{cm}^{-1}$ . However, this absorption is seldom observed due to its low absorptivity and the presence of the  $\text{CH}_2$  combination bands.

Although similar profiles are seen, the positions of both the methyl asymmetrical and symmetrical fundamental peaks varied depending on branch type for the samples examined. For example, using Fourier self deconvolution spectroscopy (Fig. 2a and b), we noted a slight peak shift for the  $\text{CH}_3$  bands to higher wavenumbers for ethyl-

Table 2

Absorptivities for the methyl asymmetrical stretch in various samples

Type	SEC area <sup>a</sup>	$\text{CH}_3\nu_a$ ( $\text{cm}^{-1}$ )	FWHH <sup>b</sup>	$\epsilon$ (l/mol/ $\text{cm}^2$ )
HMW PE	3145	—	—	—
Octacosane	2957	2960	22.1	3334
E/B	3015	2964	22.2	3444
E/H	3244	2960	22.4	3285

<sup>a</sup> Chromatograms generated using the root mean square absorbance over the  $3000\text{--}2700$   $\text{cm}^{-1}$  spectral region. Total area under SEC curve divided by sample concentration.

<sup>b</sup> From peak fitted spectra. Methyl content in samples  $\sim 70$  Me/1000 TC.

branched samples compared to butyl-branched samples. Also noted was a broadening of the  $2930\text{--}2980$   $\text{cm}^{-1}$  peak for the branched resins compared to the spectrum of an *n*-alkane having the same level of methyl content. Similar shifts in the  $\text{CH}_3\nu_a$  peak were also noted in similarly derived spectra of poly(1-butene) and poly(1-hexene). The positions of the methyl asymmetrical fundamental peak determined from derivative spectroscopy for these polymer structures are given in Table 1.

The differences in vibrational frequencies observed in the spectra of these resins are believed to be a result of mass effects rather than change in molar absorptivity. When one nonpolar group is substituted by another, the overall change in dipole moment, i.e. its 'intensity' is generally not affected [16]. Support for this assessment comes from studies that addressed the effects of structural variations on the molar absorptivities for the stretching modes (Table 2). Notable from Table 2 is that the normalized areas under the SEC curves (absorption/concentration) are essentially independent of the sample's microstructure (ca. 4% variation). This observation supports using the FTIR detector in this region of the spectrum as a concentration detector for SEC analysis. Also presented in Table 2 are the integrated molar absorptivities for the methyl asymmetric bands in these samples. As previously described, the molar absorptivities for methyl moieties attached as chain ends on *n*-alkanes and short chain branches are experimentally equivalent. More detailed studies of what spectral complexities might arise in

Table 1

Peak maxima of fundamental vibrations in selected homopolymer and ethylene 1-olefin samples estimated from second derivative spectroscopy (original spectra obtained from SEC-FTIR analysis)

Sample	Me/1000 TC	$\text{CH}_3 \nu_a$ ( $\text{cm}^{-1}$ )	$\text{CH}_2 \nu_a$ ( $\text{cm}^{-1}$ )	$\text{CH}_3 \nu_s$ ( $\text{cm}^{-1}$ )	$\text{CH}_2 \nu_s$ ( $\text{cm}^{-1}$ )
HMW PE	0	—	2927	—	2855
Octacosane	71	2960	2928	2874	2855
E/B	68	2964	2928	2876	2855
PB <sup>a</sup>	250	2963	2931 (s), 2918	2876	2856
PB + PE <sup>b</sup>	70	2964	2928	2876	2856
E/H	69	2960	2928	2874	2855
PH	167	2959	2929	2874	2855
PH + PE <sup>b</sup>	70	2960	2928	2874	2855

<sup>a</sup> Two peaks detected in  $\text{CH}_2 \nu_a$  region. One peak may be due to  $\text{CH}_2$  alpha to  $\text{CH}_3$ .

<sup>b</sup> Digitally added spectra, ethylene 1-olefin plus HMW PE (see Section 2).

resins containing other branch lengths, as well as the effects of branch proximity (e.g. density of branching and hydrodynamic volume effects) are currently underway.

### 3.2. Quantifying methyl content using C–H stretching absorptions

A number of researchers have used C–H stretching absorptions to characterize both hydrocarbon mixtures and polyolefins in terms of functional group absorptivity [13,15,17] and branching content [4–7]. In these latter studies, some type of peak deconvolution and/or ratio methods are used that focus on the methyl and methylene peaks at 2958 and 2928  $\text{cm}^{-1}$ , respectively. One common problem experienced by these methods is the presence of spectral artifacts (e.g. ghost peaks from oversubtraction or deconvolution) that reduces the method's accuracy. This is not surprising considering the observed shifts in peak position of the  $\text{CH}_{3\text{va}}$  and the changing intensity of the  $\text{CH}_{2\text{va}}$  peak in resins with different levels and types of short chain branching. Moreover, in PE resins with densities higher than 0.95 g/cc (i.e. low levels of SCBs) these techniques are difficult to apply due to the low intensity of the  $\text{CH}_{3\text{va}}$  peak compared to the large absorption of the  $\text{CH}_{2\text{va}}$  peak.

One way to circumvent many of the above problems is by the use of chemometric methods. This multivariate statistical technique, which mathematically treats the whole stretching region, captures all the spectral changes that correlate with the concentration of methyl groups present in that sample. Since the whole spectrum is used in the correlation, spectral artifacts caused by data manipulation are minimized. Another advantage offered by this methodology, is that predicted SCB values are assigned a calculated accuracy based on the statistical analysis of the spectrum.

The first step in the application of this methodology is to generate a calibration model that correlates the sample's FTIR spectra to its known methyl content (see Section 2.3). The sample training set used to generate a calibration model should contain samples similar to those that will be analyzed. For example, for the analysis of ethylene 1-hexene resins that may have in situ formed ethyl branches, the training set (Table 3) used contained samples with chain-end methyls (i.e. *n*-alkane and homopolymer fractions) as well as ethyl and butyl short chain branches (ethylene 1-olefin copolymers).

In each sample, 32 absorbance values (every fourth wavenumber) are initially analyzed over a 2996–2836  $\text{cm}^{-1}$  spectral range. A correlation between the absorption values and the level of methyl moieties measured by NMR (or estimated by  $M_n$ ) for each sample is subsequently calculated using the algorithms provided by the chemometric software. The resulting analysis indicates that three sets of combined absorbance bands (principal components) capture the majority of spectral variance (99.92%) that is correlated to methyl content in these samples. The absorption bands that

Table 3  
Training set used to construct calibration model

Sample #	Total methyls measured <sup>a</sup>		Mol% SCB <sup>c</sup>	
	(Me/1000 TC)	Methyl type <sup>b</sup>	Ethyl	Butyl
1	0.5	CE	–	–
2	1.3	CE	–	–
3	1.4	CE + SCB	0.2	–
4	1.6	CE	–	–
5	1.7	CE	–	–
6	1.8	CE + SCB	0.2	–
7	2.0	CE	–	–
8	2.2	CE	–	–
9	2.7	CE	–	–
10	3.3	CE	–	–
11	3.5	CE + SCB	0.2	–
12	3.7	CE	–	–
13	4.2	CE	–	–
14	4.3	CE + SCB	–	0.9
15	8.2	CE + SCB	–	1.6
16	9.4	CE + SCB	0.1	0.2
17	10.8	CE + SCB	0.7	1.5
18	11.1	CE + SCB	0.1	2.1
19	13.1	CE + SCB	–	2.6
20	13.3	CE + SCB	0.8	1.8
21	15.2	CE + SCB	0.9	2.2
22	15.4	CE + SCB	–	2.8
23	16.6	CE + SCB	–	3.4
24	21.5	CE	–	–
25	39.8	CE	–	–
26	62.1	CE	–	–
27	82.7	CE	–	–

<sup>a</sup> SCB + CE = short chain branches and chain end methyls; CE = chain end methyls.

<sup>b</sup> Values obtained by NMR for samples with SCB + CE methyls; values for samples containing only CE methyls were calculated from  $M_n$  (see Section 2).

<sup>c</sup> Calculated from NMR measured samples.

dominate the variance in each principal component were determined by examining the spectral loadings (Table 4). The bands given in Table 4 are those expected in light of the spectral differences previously noted for the various branch types (Fig. 2) and aptly demonstrate the physical basis behind the methodology employed. Predicted vs. actual values for the training set are plotted in Fig. 3. The cross-validated, calibration model shows an excellent correlation (RSQ = 0.999) between the predicted and actual values.

Table 4  
Factors and dominant absorption bands

Factor	% Variance accounted for	SEV <sup>a</sup>	Dominant absorption bands ( $\text{cm}^{-1}$ ) <sup>b</sup>		
1	98.40	3.23	2959	2906	2874
2	1.06	0.74	2962	2927	2854
3	0.46	0.53	2945	2907	2868

<sup>a</sup> Standard error of validation.

<sup>b</sup> Obtained from loadings plots for each factor.

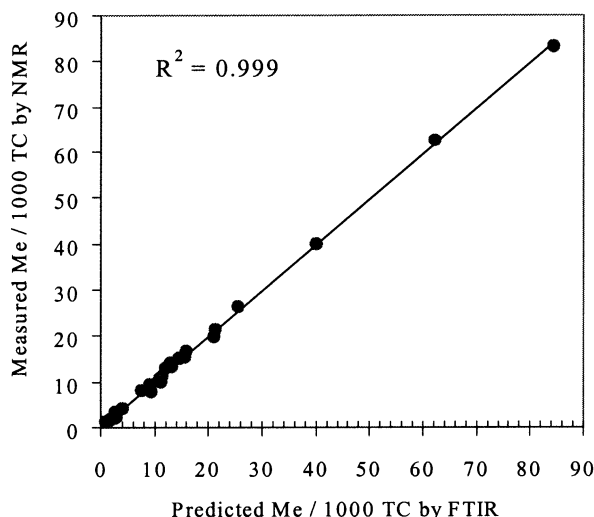


Fig. 3. Predicted vs. actual values for training set.

The standard error of validation (SEV) for this training set was  $\pm 0.5$  Me/1000 TC (ca. 0.1 mol%).

The applicable predictive range for this particular model with regards to branch type was estimated by analyzing digitally generated spectra containing ethyl and butyl branches. The difference between the predicted and known methyl levels for these samples are plotted in Fig. 4. From the equation derived from a least square fit of the data, it appears that methyl content can be accurately predicted (i.e.  $3\sigma$ , where  $\sigma = 0.5$ ) up to 15 Me/1000 TC from spectra representing samples containing mainly butyl branches. However, as the methyl content increased, the model over-predicted the methyl level for the sample. Conversely, a similar analysis of spectra representing samples that contain mainly ethyl branches shows an underestimation of branch level after about 6 Me/1000 TC. In copolymers containing

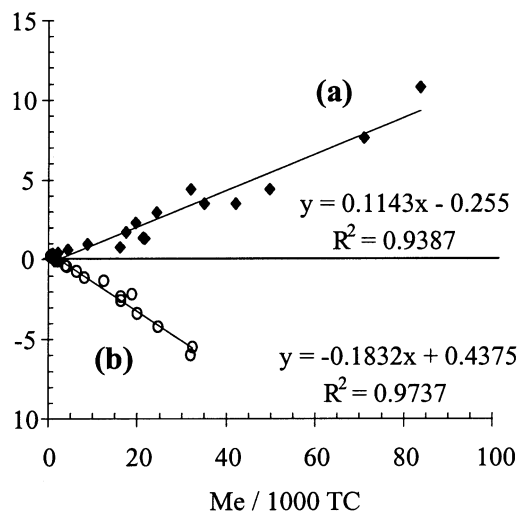


Fig. 4. Variance in predicted values for butyl branches (curve a) and ethyl branches (curve b).

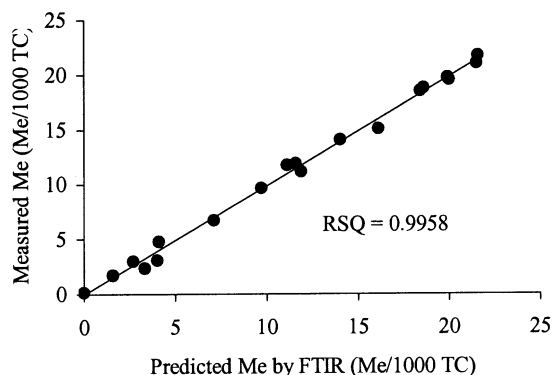


Fig. 5. External validation of the model terms of Me/1000 TC.

both branch types, the accuracy decreases ( $>3\sigma$ ) in resins with ethyl/butyl SCB ratios greater than 0.5.

The limits of this particular model are not surprising considering the sample composition of the training set (Table 3). The absence of samples having branch levels above the critical concentrations of branching (i.e.  $\sim 15$  and 6 Me/1000 TC), lead to spectral profiles that were not accurately accounted for by the model. The predicted ability of this model can be further extended by incorporating the appropriate samples into the calibration set. However, as the model is made more robust, an increase in both the number of principal components and predictive uncertainty are expected (e.g. the same methyl levels can arise from very different spectral profiles). Conversely, highly accurate but limited models can be generated for each branch type. Alternately, if the branch type of the sample is known, the measured results could be adjusted using the relationships given in Fig. 4.

The predictive validity for the calibration model generated from samples in Table 3 was further tested by analyzing spectra acquired from an additional set of 18 samples with methyl contents between 0 and 23.6 Me/1000 TC. External validation of the model in terms of Me/1000 TC is illustrated in Fig. 5. From these data the predictive error in the determination of methyl levels in whole polymer samples was estimated to be  $\pm 0.43$  Me/1000 TC. This value is in good agreement with the SEV, previously calculated from cross validation of the training set. We expect the above model to be particularly applicable to high density, ethylene 1-olefin resins.

### 3.3. SCB analysis across the MWD

Having established a working predictive model, the next step of this analysis was to obtain SCB information over as much of the MWD as possible. To achieve this end, both spectral and chromatographic concentration limits need to be addressed. With regard to spectral concentrations, the number of spectra classified as outliers needs to be minimized. For example, as sample concentration at the FTIR detector decreases, a critical concentration will be reached

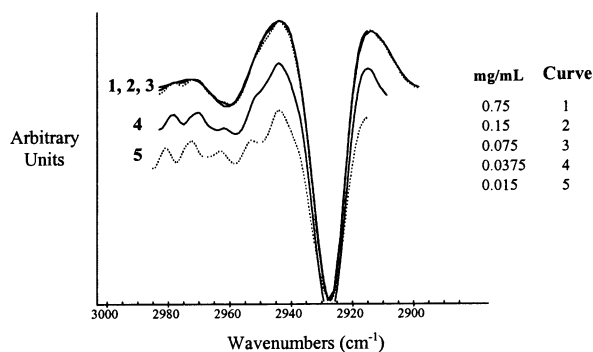


Fig. 6. Second derivative spectra for the tetracosane at various concentrations. Changes in the spectral integrity for  $\text{CH}_3$  ( $\sim 2960 \text{ cm}^{-1}$ ) and the  $\text{CH}_2$  ( $\sim 2928 \text{ cm}^{-1}$ ) asymmetric stretches are shown.

at which the measured spectra are no longer representative of sample spectra obtained at higher concentrations. That is, the relationships between absorption bands have changed due to increased spectral noise. This point is illustrated using second derivative spectra for various concentrations of tetracosane (Fig. 6).

In Fig. 6, the changes in the spectral integrity for the  $\text{CH}_3$  ( $\sim 2960 \text{ cm}^{-1}$ ) and the  $\text{CH}_2$  ( $\sim 2928 \text{ cm}^{-1}$ ) asymmetric stretches that occur with decreasing concentration are shown. A visual inspection of these spectra suggests that spectral integrity is maintained when sample concentration at the detector is  $\geq 0.075 \text{ mg/ml}$ . Similar results were found for the SEC–FTIR analysis of HDPE ( $\rho = 0.948 \text{ g/cc}$ ) as shown in Table 5. This data demonstrates that a lack of fit to the predictive model occurs at concentrations between 0.06 and 0.07 mg/ml. At these concentration limits,  $\geq 90\%$  of the sample's MWD was quantified. A greater portion of the MWD can be analyzed in samples with narrower MWDs (i.e.  $M_w/M_n < 22$ ). Also, values for the concentration limits at either end of the chromatogram are influenced by peak symmetry of the chromatogram (i.e. the steeper slope across a time slice, the greater the concentration change in each subsequent time slice). One additional point to note is that a breakdown in spectral integrity (relationships between absorption bands) will significantly affect the quantifying of SCB levels (as described above) before it influences the

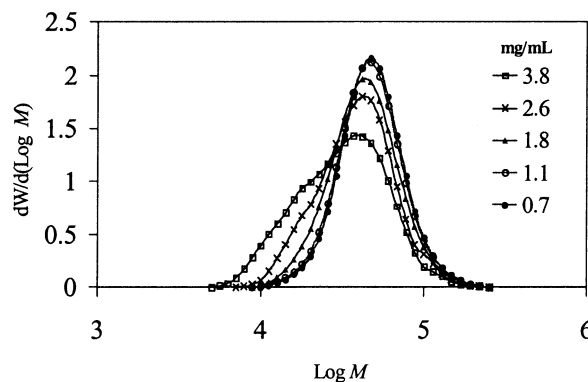


Fig. 7. Loss in chromatographic resolution for a narrow molecular weight sample (MWD = 1.1) due to column overload.

linearity of FTIR detector signal vs. the amount of solute injected.

For MW analysis using SEC, low injection volumes ( $220 \mu\text{l}$ ) and sample concentrations ( $1.0\text{--}1.8 \text{ mg/ml}$ ) are typically used. For SCB studies conducted using online SEC–FTIR [4–7], larger injection volumes ( $400\text{--}1000 \mu\text{l}$ ) and higher sample concentrations ( $\geq 2.0 \text{ mg/ml}$ ) have been used in order to obtain sufficient amounts of sample for FTIR analysis. Because such high injection volumes and sample concentrations are typically used, one concern that arises is that column overloading may occur (i.e. the column is no longer separating the sample based on molecular weight).

The types of chromatographic distortions caused by column overloading are illustrated in Fig. 7 for a narrow molecular weight sample. The observed distortions of the SEC curves as sample concentration increases (i.e. peak elution volumes shift to higher values with increasing solute concentration) are artifacts caused by increased viscosity, coil shrinkage and osmotic effects [18]. All of these effects increase as the sample's molecular mass increases, heterogeneity decreases, and the resolution power of the columns become higher.

Experiments to determine acceptable ranges of chromatographic parameters, particularly injection volume and concentration of the injected solution, were conducted

Table 5  
Concentration effects in SEC–FTIR analysis of a HDPE ( $\rho = 0.948 \text{ g/cc}$ ) sample

Slice number <sup>a</sup>	Times (min)	Portion of chromatograph	Mg/ml	Probability <sup>b</sup>
1	10.30–10.42	HMW tail	$\sim 0$	1
16	11.97–12.09	HMW tail	0.048	1
17	12.09–12.21	HMW tail	0.055	0.97
45	15.44–15.56	Peak	0.152	0.67
67	18.07–18.19	LMW tail	0.066	0.98
68	18.19–18.31	LMW tail	0.056	1
77	19.27–19.39	LMW tail	$\sim 0$	1

<sup>a</sup> FTIR spectra co-added in each slice (16 scans).

<sup>b</sup> Spectra with values  $>0.99$  were considered outliers.

Table 6  
SEC analysis of a narrow molecular weight ethylene 1-olefin sample (solvent gradient fraction at 1.1 mg/ml concentration)

	$M_n$ (kg/mol)	$M_w$ (kg/mol)	$M_z$ (kg/mol)	$M_p$ (kg/mol)	$M_w/M_n$
SEC <sup>a</sup>	108	121	138	110	1.13
SEC-FTIR <sup>b</sup>	99	120	146	108	1.21
	97	120	148	108	1.24
	98	119	146	108	1.21

<sup>a</sup> Using a 220  $\mu$ l injection volume on two PL Mixed B columns.

<sup>b</sup> Using a 500  $\mu$ l injection volume on two PL Mixed A columns.

using narrow (PE fraction) and broad molecular weight homopolymers. We found that adequate chromatographic resolution is maintained by using a 500  $\mu$ l loop and concentrations of 1.6 and 1.1 mg/ml for broad molecular weight ( $M_w/M_n = 22$ ) and narrow molecular weight ( $M_w/M_n = 1.1$ ) samples, respectively. These values correspond to about twice the load (i.e. sample weight applied to column) typically used for SEC analysis. When the spectral concentration limits are imposed on the SEC concentration requirements, we find that accurate  $M_w$  values (<10% variation from those results using low injection volume and loads conditions) can be obtained. However, values for  $M_n$  are lower than those found using typical SEC conditions and subsequently higher molecular weight dispersities result. The magnitude of the latter deviations is dependent on the sample's molar mass and initial dispersity. Typical molecular weight values obtained from the SEC-FTIR analysis are illustrated for the analysis of a narrow molecular weight ethylene 1-olefin sample given in Table 6.

In the cited SCB studies using online SEC-FTIR [4–7], molecular weight data are obtained using typical SEC conditions (DRI detection, low injection volumes, etc.) followed by superimposing SCB data acquired using vastly different chromatographic conditions. It is evident from our studies that this approach has many pitfalls, one of which is the assignment of SCB values to the wrong MW region (MW data which arises from artifacts in the analysis). Although, our current method of SEC analysis is not completely optimized, we believe that a more accurate assessment of the sample's SCB profile is provided when the microstructure and molecular weight data are obtained under the same chromatographic conditions. Studies to optimize SEC aspects of this method (e.g. higher analysis temperatures, mixed particle size in columns, etc.) will be the subject of future publications.

One aspect of SCB analysis by SEC-FTIR not commonly addressed in reported studies is the error associated with individual data points. As previously shown (Table 5), an examination of the spectral residuals given for spectra acquired across the chromatogram shows that the largest error (lack of fit) occurs at the tails of the MWD. Subsequent analysis of replicate runs (Fig. 8a) confirms this assessment. The lack of fit results from low signal to noise ratios caused by low concentrations. Although methods have been developed to estimate the error in individual data points predicted

using chemometric techniques [19], in this analysis they are inapplicable, since they assume no concentration variation in the spectra measured. This is clearly not the case in this analysis.

In this study, data error was first assessed by utilizing the statistical analysis generated from the chemometric model that flags outlier data that is greater than 0.99 probability (Fig. 8b). Although a constant error based on validation studies could be assigned to the remaining data, this approach does not adequately reflect the variance in the data across the MWD as described above. To better capture this variance, we have empirically estimated the error limits

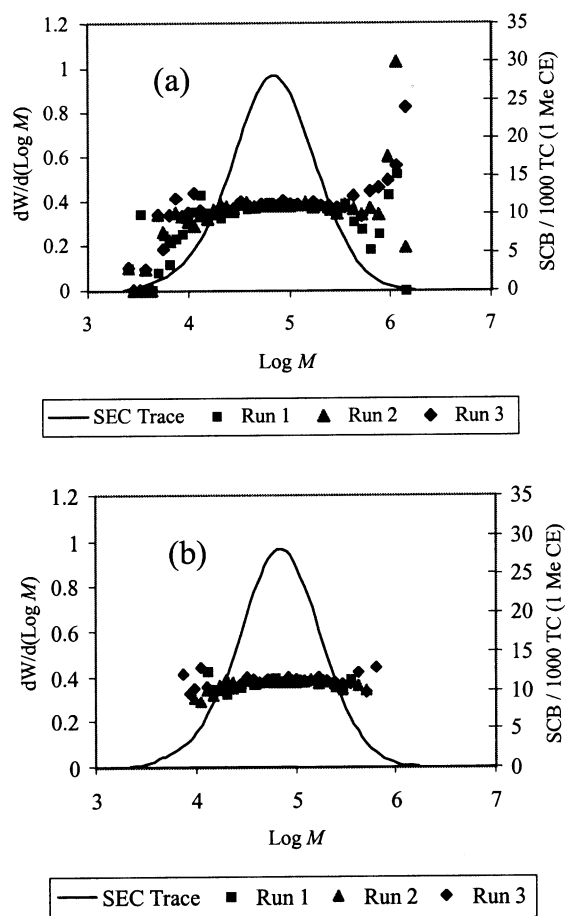


Fig. 8. Analysis of replicate runs (a); flagged outlier data greater than 0.99 probability (b).



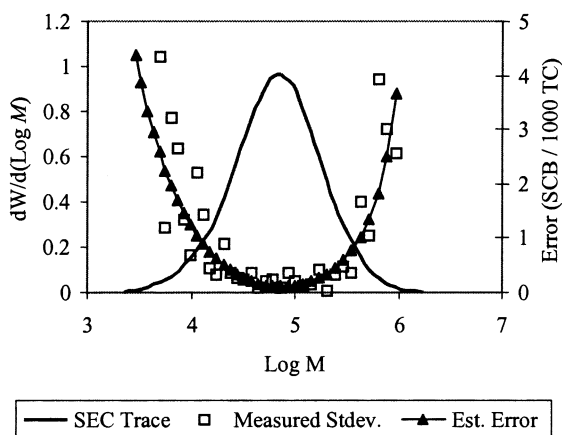


Fig. 9. Precision in replicate runs. Estimated error =  $1.89 \cdot [\text{spectral area}]^{-1/2} - 0.58$ .

for the measured branch levels in individual time slices of the chromatogram in terms of SCB/1000 total carbons. This was done by noting that the precision in replicate runs varied linearly with the inverse square root of the spectral area (Fig. 9) and was applicable over the range of SCB levels studied. Although the precision of this method is very good at the sample's concentration maximum ( $\pm 0.1$  Me/1000 TC), the minimum error allowed in a typical analysis was  $\pm 0.5$  Me/1000 TC. This value is based on

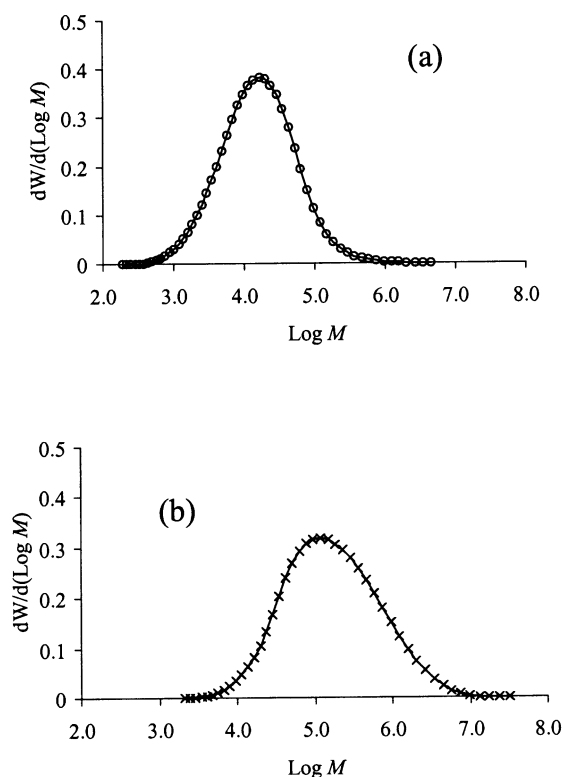


Fig. 10. Molecular weight profiles for the blend components (a) LMW homopolymer (0 Me/1000 TC) and (b) HMW branched, ethylene 1-hexene copolymer (2.9 Me/1000 TC).

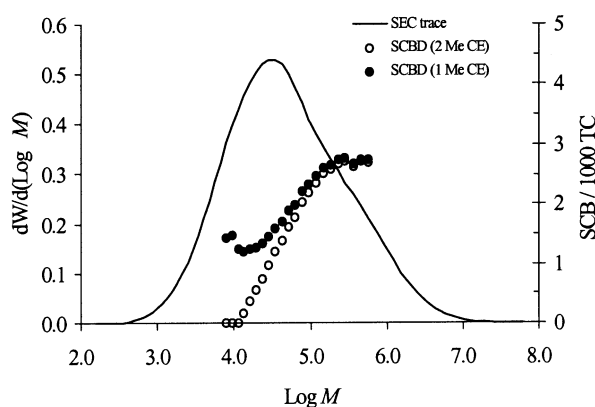


Fig. 11. Blend molecular weight profile and its SCB distribution measured by SEC–FTIR.

the predicted error determined from the cross and external validation studies described above. We used this approach to estimate the error for a single run.

### 3.4. Application of method

As a final evaluation of our SEC–FTIR method, two polyolefin samples with known composition and microstructure were analyzed. In the first study, a solution blend composed of a low molecular weight homopolymer mixed in equal portions with a branched ethylene 1-hexene copolymer was analyzed. The molecular weight profiles for the blend components are given in Fig. 10. The measured SCB level (2.9 SCB/1000 TC) in the HMW component was taken to be constant across the MWDs (i.e. a flat SCBD). Analysis of the HMW component by SEC–FTIR supports this assessment (data not shown). The molecular weight profile for the blend and its SCB distribution measured by SEC–FTIR are given in Fig. 11. Analysis of this bimodal resin as shown in Fig. 11 illustrates the importance of properly choosing the correct number of methyl chain ends. Typically, end group contributions (and subsequent corrections) are negligible after the molecular

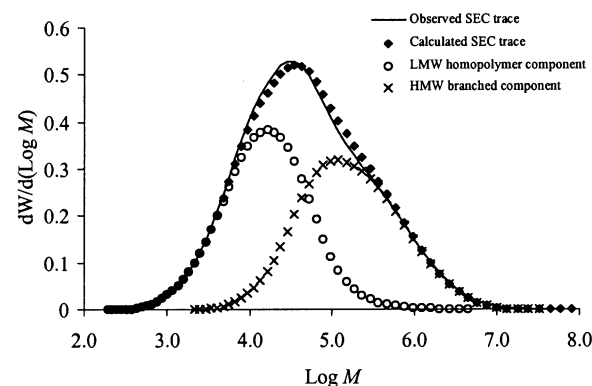


Fig. 12. Actual SEC blend trace and SEC blend trace generated from SEC curves measured for the two components.

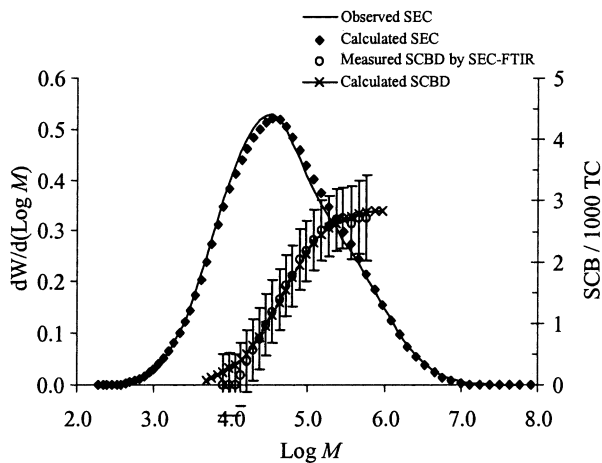


Fig. 13. Calculated SCB levels for blend compared to the SCB levels from SEC-FTIR analysis of the actual blend.

weight reaches  $\sim 15,000$ . In this sample, both resins were known to contain only methyl chain ends.

The accuracy of the SCB analysis for the blend can be checked, by comparing the SEC-FTIR results to those calculated using the individual components. For example, a SEC trace for the blend can be generated, by adding together the SEC curves measured for the two components. The resulting SEC trace (Fig. 12) compares well with the SEC trace measured for the actual blend. In a similar manner, the SCB levels for the blend were calculated and compared to the SEC-FTIR analysis of the actual blend. As shown in Fig. 13, an excellent correlation between the two was found. From the analysis of this resin, one can readily see the problem that column overload would create when attempting to interpret the results. This latter figure also illustrates the power of this method to elucidate polymer architecture in certain multi-modal systems. However, the ability of SEC-FTIR analysis to discern a sample's compositional heterogeneity is dependent upon the extent to which the MWD of its components overlap.

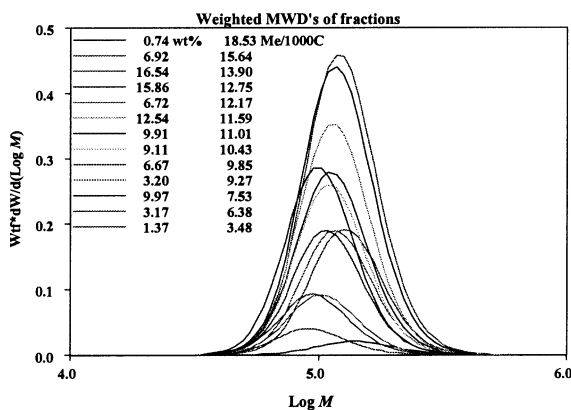


Fig. 14. Overlay of the molecular weight data and SCB levels for isolated PTREF fractions of an ethylene 1-olefin sample.

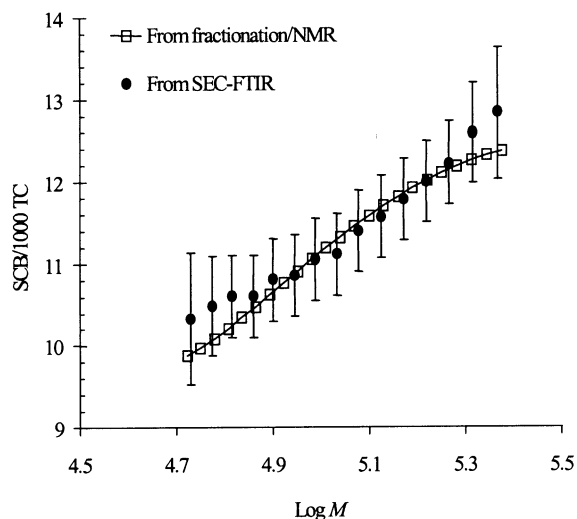


Fig. 15. SCB levels determined from SEC-FTIR and results obtained using typical PTREF techniques and NMR analysis.

This latter point is illustrated in the second sample studied where a direct comparison was made between SCB levels determined from SEC-FTIR and results obtained using typical fractionation techniques and NMR analysis. Preparative Temperature Rising Elution Fractionation (PTREF) samples of the ethylene 1-olefin sample given in Table 6 were collected and subsequently analyzed by conventional SEC and NMR in order to assign molecular weights and SCB levels to each fraction. An overlay of the weighted molecular weight data and SCB levels for the isolated fractions is shown in Fig. 14.

The SCB distribution across the MWD in the parent resin was reconstructed by accounting for SCBs contributed by each fraction. In Fig. 15, the reconstructed SCB distribution across the MWD of this resin was compared to results obtained by SEC-FTIR analysis of the parent resin. As shown for this sample, a good correlation was found to exist between the two methods. Both methods show the expected increase in branch content with increasing molecular weight based on the solvent/non-solvent pair used for the solvent gradient fractionation [20]. Although the rise in branching level in this sample was slight ( $\sim 10$ – $12$  SCB/1000 TC), the trend could be observed using the SEC-FTIR method. However, from this study it is evident that characterization of the parent resin by SEC-FTIR did not fully elucidate the sample's compositional heterogeneity. In the SEC-FTIR characterization of a resin, the average branch content is measured in each slice of the MWD. Because the molecular weights of the fractions were very similar (unlike the previous blend sample), SEC-FTIR analysis could not discern the apparent compositional heterogeneity in the parent resin. Similar results have been reported by Falidi and Soares [3] in studies using offline SEC-FTIR analysis of ethylene 1-olefins.

#### 4. Conclusions

A prototype method for the SEC–FTIR analysis of SCBD across the MWD has been developed. The predicted SCB versus molecular weight profiles obtained by this method were verified through the analysis of samples with known composition and microstructure. The current prototype method uses the 3000–2700  $\text{cm}^{-1}$  spectral region and provides SCB profiles with sufficient precision to detect trends resulting from catalyst and process changes. Chromatographic conditions were found which maximize sample concentration at the detector while maintaining acceptable resolution. Using chemometric techniques, spectra from individual time slices of the chromatogram were successfully analyzed for co-monomer branch levels in terms of total methyl content and subsequently converted to SCB by estimating molecular chain end contributions. In general, the composition of the training set in terms of branch type and level dictated the accuracy of this method. The precision of SCB values measured for each time slice varied across the MWDs due to errors that arises from concentration effects (i.e. highest error at the tails of the chromatogram due to low signal to noise). Techniques were successfully developed to assess the additional error associated with concentration effects.

The specific application of this method showed that, using a single calibration curve, SCB levels were accurately predicted within  $\pm 0.5/1000$  total carbons (i.e. ca. 0.1 mol%) in resins that contained ethyl and/or butyl branches. However, in this particular model which was used to exemplify the general method, the analysis is limited to resins with  $\leq 6$  SCB/1000 TC ethyl branches and  $\leq 15$  SCB/1000 TC butyl branches. We conclude that the current method provides SCB versus MWD profiles with sufficient precision to detect trends resulting from catalyst and process changes even in HDPE samples.

#### Acknowledgements

The authors would like to thank the following people for the contributions to this work: Dr Chung C. Tso for supplying fractionated polymer samples, Dr Antoni Jurkiewicz for conducting polymer NMR analysis, and Drs Alen Eastman and Jason Gislason for their assistance with chemometric techniques. Lastly, the authors would like to thank Chevron Phillips Chemical Company for its support of this work.

#### Appendix A

The calibration from chemometrics gives  $N_T$ , the total number of methyls measured per 1000 total carbon molecules (per 1000 TC). To obtain  $N_{\text{SCB}}$ , the number of short chain branches per 1000 TC, we must subtract  $N_E$ , the

number of methyl end groups per 1000 TC at a given molecular weight,  $M$ .

$$N_{\text{SCB}} = N_T - N_E \quad (\text{A1})$$

At any given molecular mass,  $M$ , the total number of carbons would seem to depend on both the number of methyl end groups and the number and length of any short chain branches (that are all assumed to be terminated by a methyl group). However, we see that the presence of a SCB off the main chain replaces one of the hydrogen atoms from a  $\text{CH}_2$  with a carbon chain where each carbon except the end carbon has two hydrogen atoms associated with it. If the third hydrogen from the end carbon is associated with the carbon at the branch point (for mass counting purposes only), then all the carbons on the backbone and in the short chain branches of any length have two hydrogen atoms associated with them. Therefore,

$$14n_1 + 15n_2 = M, \quad (\text{A2})$$

where  $n_1$  is the number of  $\text{CH}_2$ -equivalent carbons per molecule of mass  $M$  and  $n_2$  is the number of  $\text{CH}_3$  chain-end carbons per molecule of mass  $M$  only (that is, not including the ends of short chain branches). Only one end can be a vinyl end group instead of a methyl end group so that  $n_2$  can be either 1 or 2 for any given molecule. For a collection of molecules of mass  $M$ ,  $n_2$  can take on any value between 1 and 2.

Eq. (A2) can be solved for the number of  $\text{CH}_2$  carbons in terms of the number of  $\text{CH}_3$  end group carbons.

$$n_1 = (M - 15n_2)/14 \quad (\text{A3})$$

An expression valid for homopolymers and copolymers (even with mixed lengths of short chain branches) for the total number of carbons in a molecule of mass  $M$  with  $n_2$  methyl end groups can therefore be written as

$$n_1 + n_2 = (M - n_2)/14 \quad (\text{A4})$$

Since calibration is per 1000 TC,  $N_M$ , the number of molecules of molecular mass  $M$  with  $n_2$   $\text{CH}_3$  end groups in 1000 TC is

$$N_M = 1000/(n_1 + n_2) = (1000)(14)/(M - n_2) \quad (\text{A5})$$

Finally,  $N_E$ , the number of chain-end methyls in 1000 TC at a molecular mass  $M$  is given by  $n_2$ , the number of chain-end methyls per molecule, times the number of molecules in 1000 TC,  $N_M$ , to give

$$N_E = n_2 \times (1000)(14)/(M - n_2). \quad (\text{A6})$$

In all cases of interest,  $M \gg n_2$  so that

$$N_E = 14,000n_2/M \quad (\text{A7})$$

The number of chain-end methyls,  $n_2$ , can also be expressed as  $2 - V_{\text{CE}}$ , where  $V_{\text{CE}}$  is the number of vinyl chain ends per molecule to give

$$N_E = 14,000(2 - V_{\text{CE}})/M. \quad (\text{A8})$$

## References

- [1] Soare JBP, Abbott RF, Kim JD. *J Polym Sci, Part B: Polym Phys* 2000;38:1267.
- [2] Willis JN, Wheeler L. *Adv Chem Ser* 1995;247:253.
- [3] Faldi A, Soares JBP. *Polymer* 2001;42:3057.
- [4] Housaki T, Satoh K, Nishikida K, Morimoto M. *Makromol Chem, Rapid Commun* 1988;9:525.
- [5] Nishikida K, Housaki T, Morimoto M, Kinoshita T. *J Chromatogr* 1990;20:517.
- [6] Markovich RP, Hazlitt LG, Smith-Courtney L. *ACS Symp Ser* 1993;521 (Chromatography of Polymers).
- [7] Rose LJ, Frye CJ, Blyth SM. *Charact. Copolym, Book Pap. One-Day Semin.* Shrewsbury, UK: Rapra Technology, 1995. p. 1–8, paper 5.
- [8] Jordens K, Wilkes GL, Janzen J, Rohlfing DC, Welch MB. *Polymer* 2000;41:7175.
- [9] Grushka E, Monacelli GC. *Anal Chem* 1972;44:484.
- [10] Randall JC, Hseish ET. In: Randall JC, editor. *NMR and macromolecules; sequence, dynamic, and domain structure*, ACS symposium series 247. Washington, DC: American Chemical Society, 1984.
- [11] Witt DR. In: Jenkins AD, Ledwith A, editors. *Mechanism and structure in polymer chemistry*. New York: Wiley, 1974. Chap. 13.
- [12] Lenz RW. *Organic chemistry of synthetic high polymers*. New York: Wiley, 1967. Chap. 15.
- [13] Fox JJ, Martin AE. *Proc R Soc Lond* 1937;162:419.
- [14] Nielsen JR, Woollett AH. *J Chem Phys* 1956;26:1391.
- [15] Zenker W. *Anal Chem* 1972;44:1235.
- [16] Hummel DO. *Vib Spectrosc Appl Infrared Spectrosc Monogr Mod Chem* 1974;6:112–50.
- [17] Wiberley SE, Bruce SC, Bauer WH. *Anal Chem* 1960;32:217.
- [18] Glocker G. *Polymer characterization by liquid chromatography*. *J Chromatogr Library* 1987;34.
- [19] ASTM Method E 1655.
- [20] Hsieh ET, Tso CC, Byers JD, Johnson TW, Fu Q, Cheng SZD. *J Macromol Sci Phys* 1997;B36(5):615.